

Metallocene-mediated synthesis of chain-end functionalized polypropylene and application in PP/clay nanocomposites

T.C. Chung *

Department of Materials Science and Engineering, The Pennsylvania State University, 325 Steidle Building, University Park, PA 16802, USA

Received 10 January 2005; revised 12 February 2005; accepted 18 April 2005

Available online 8 June 2005

Abstract

This paper summarizes our research in the preparation of chain end functionalized isotactic polypropylene (PP) having a terminal functional group, such as Cl, OH, and NH₂. The chemistry involves metallocene-mediated propylene polymerization using *rac*-Me₂Si[2-Me-4-Ph(Ind)]₂ZrCl₂/MAO complex in the presence of styrene derivatives (St-f) and hydrogen, which serve as the chain transfer agents. The molecular weight of the resulting PP polymers with a terminal Cl, OH and NH₂ group (i.e., PP-t-Cl, PP-t-OH and PP-t-NH₂) are inversely proportional to the molar ratio of [St-f]/[propylene]. Despite the extremely low concentration of functional group, the high molecular weight chain end functionalized PP-t-OH and PP-t-NH₃⁺ exhibit a distinctive advantage over other functional PP polymers containing side chain functional groups or long functional blocks. The terminal hydrophilic OH and NH₃⁺ cations, with good mobility and reactivity, effectively hydrogen bond and ion-exchange the cations (Li⁺, Na⁺, etc.) located between the clay interlayers, respectively. Such interactions anchor the PP chain to the clay surfaces. On the other hand, the remaining rest of the unperturbed end-tethered high molecular weight PP tail exfoliates the clay layers. This exfoliated structure is maintained even after further mixing of the PP-bearing platelets with pure neat PP polymers.

© 2005 Elsevier B.V. All rights reserved.

Keywords: Functionalization; Polypropylene; Metallocene; Nanocomposite; PP/clay composite

1. Introduction

Ever since the discovery of Ziegler–Natta catalysts in the early 1950s the functionalization of polyolefin (i.e. PE, PP, EP, s-PS, etc.) has long been a scientifically interesting and technologically important subject [1]. The lack of functionality in polyolefins, resulting in poor compatibility with other materials, has been a major drawback in many applications, particularly those in which adhesion, dyeability, printability, or compatibility with other polymers is paramount.

The chain-end functionalized polymer is a very attractive polymer structure that possesses an unperturbed polymer chain structure and desirable physical

properties (such as melting temperature, crystallinity, glass transition temperature, melt flow, etc.) that are almost the same as those of the pure polymer. Nevertheless, the terminal reactive group at the polymer chain end has good mobility and can provide a reactive site for many applications, such as adhesion to the substrates [2] and reactive blending [3] to improve the compatibility of two dissimilar polymer blends. This chain end functionalized polymer structure is particularly useful in polyolefin, whose lack of functionality and poor compatibility with other materials has imposed limitations on its applications [4].

In chemistry, the preparation of chain end functionalized polymers has been largely limited to living polymerization with the use of an initiator bearing a functional group [5] or a control termination (functionalization) reaction [6] of the living polymer chain end.

* Tel.: +1 814 863 1394; fax: +1 814 865 2917.

E-mail address: chung@ems.psu.edu.

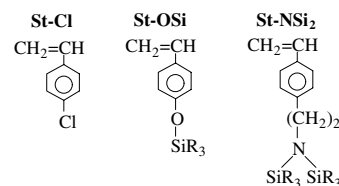
Unfortunately, there are only a few Ziegler–Natta type transition metal coordination catalysts that exhibit living polymerization behavior, and most of them are limited to the preparation of polyethylene and poly-(1-hexene) cases [7]. Furthermore, living polymerization only produces one polymer chain per initiator, which presents a relatively low rate of catalyst activity in the typical polyolefin preparation.

In our previous papers [8], we have reported a new chemical route to prepare polyolefin (including PE, PP, s-PS, etc.) with a terminal reactive group and obtain high catalyst activity. The chemistry is based on a chain transfer reaction involving a reactive chain transfer agent, including dialkylborane ($H-BR_2$) [9] and p-methylstyrene/hydrogen (p-MS/ H_2) [10], during metallocene-mediated olefin polymerization. All polymers formed contain a terminal borane or p-MS group and have a relatively narrow molecular weight distribution ($M_w/M_n \sim 2$). The polymer molecular weight (from a few thousand to a hundred thousand) was basically controlled by the mole ratio of [chain transfer agent]/[olefin]. Both the terminal borane and p-MS groups are very versatile, and can serve as the reactive sites for subsequent functionalization reactions or conversion to living initiators for chain extension reactions.

2. Synthesis of PP-t-Cl, PP-t-OH and PP-t-NH₂

It is very desirable to extend this chemical route to directly prepare polyolefin with a desirable terminal functional group, such as Cl, OH, and NH_2 . In other words, the ideal reaction is a one-pot in situ polymerization process [11], and no chain end functionalization would be needed after the polymerization reaction. The basic idea in the direct preparation of the chain functionalized PP was to use a functionalized styrenic chain transfer agent (St-f) as the chain transfer agent that could engage in similar metallocene-mediated propylene polymerization/chain transfer reaction under some reaction conditions. Three St-f molecules were investigated, including p-chlorostyrene (St-Cl), silane-protected p-vinylphenol (St-OSi) and silane-protected p-ethylaminostyrene (St-NSi₂), as illustrated in Scheme 1. The silane groups provide effective protection for both the OH and NH_2 functional groups during the metallocene catalysis, and they can be completely deprotected by aqueous HCl solution during the sample work-up procedure.

No external protection agent is needed for St-Cl in metallocene/MAO systems. However, the metallocene cationic site is very sensitive to the OH and NH_2 functional groups. The silane groups not only provide effective protection for both the OH and NH_2 functional groups during the metallocene catalysis, but also can be completely deprotected by aqueous HCl solution during the sample work-up procedure. The overall reaction



Scheme 1.

especially benefits from the very small quantity of the chain transfer agent needed in the preparation of high polymers. Therefore, the additional protection–deprotection step causes almost no change in the polymerization conditions and procedures.

Eq. (1) illustrates the general reaction scheme. During the course of propylene 1,2- insertion, the propagating M^+-C site (II) eventually reacts with a St-NSi₂ unit (k_{12}) (via 2,1-insertion) to form a St-NSi₂ capped propagating site (III) with an adjacent phenyl group interacting with metal cation. The new propagating site (III) is incapable of continuing the insertion of St-NSi₂ (k_{22}) or propylene (k_{21}) due to the steric jamming. However, it can react with hydrogen to complete the chain transfer reaction. This consecutive reaction with St-NSi₂ and hydrogen results in a PP-t-St-NSi₂ polymer chain (IV) and a regenerated Zr-H species (I) reinitiates the polymerization of propylene and continues the polymerization cycles. After completing the polymerization, the desirable NH_2 terminal group in PP-t- NH_2 (V) can be easily recovered during the sample work-up step using HCl aqueous solution. Theoretically, the PP-t- NH_2 molecular weight should be linearly proportion to the molar ratio of [propylene]/[St-NSi₂].

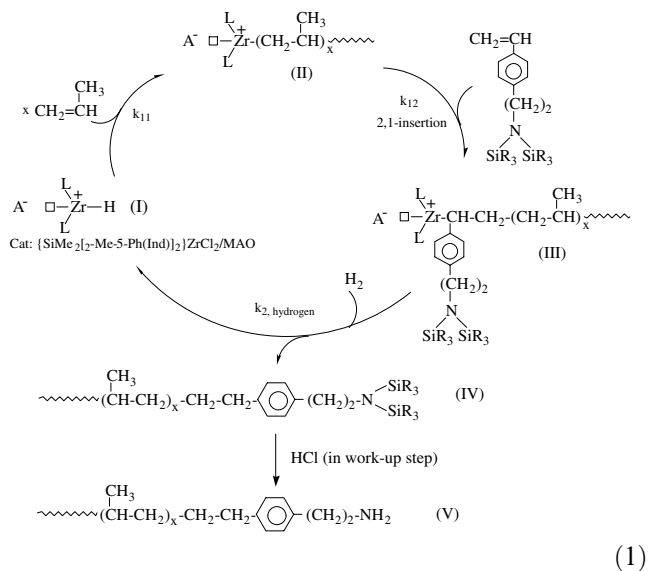


Table 1 summarize the experimental results involving St-Cl/ H_2 , St-OSi/ H_2 , and St-NSi₂/ H_2 , respectively, in *rac*-Me₂Si[2-Me-4-Ph(Ind)]₂ZrCl₂/MAO catalyzed polymerization of propylene. In all control reactions, a small

Table 1
A summary of PP-t-Cl, PP-t-St-OH and PP-t-St-NH₂ polymers^a

Run	St-f ^b (mol/l)	H ₂ (psi)	Yield (g)	Catalyst activity ^c	Cl, OH or NH ₂ in PP (mol%)	M_n ($\times 10^{-3}$)	PDI (M_w/M_n)	T_m (°C)
A-1	0.144	0	~0	~0	–	–	–	–
A-2	0.144	6	1.36	4402	0.13	45.3	1.9	159.0
A-3	0.144	12	7.56	24192	0.13	47.5	2.0	158.2
A-4	0.144	20	21.8	70435	0.12	46.1	2.1	158.1
B-1	0.289	0	~0	~0	–	–	–	–
B-2	0.289	6	1.24	4388	0.23	18.5	2.2	156.8
B-3	0.289	14	4.44	15712	0.23	19.1	2.1	157.1
B-4	0.289	20	12.91	45673	0.22	18.7	2.1	156.9
C-1	0.198	0	~0	~0	–	–	–	–
C-2	0.198	6	0.36	1165	0.09	52.1	2.3	159.1
C-3	0.198	12	2.36	7637	0.08	53.4	2.4	158.4
C-4	0.198	20	8.34	26995	0.10	52.5	2.2	158.2
D-1	0.396	0	~0	~0	–	–	–	–
D-2	0.396	6	~0	~0	–	–	–	–
D-3	0.396	12	0.63	2039	0.18	23.4	2.5	157.4
D-4	0.396	20	2.57	8318	0.20	22.0	2.0	156.3
E-1	0.125	0	~0	~0	–	–	–	–
E-2	0.125	6	0.41	1327	0.07	56.3	2.1	159.1
E-3	0.125	12	2.62	8480	0.06	55.4	2.5	158.4
E-4	0.125	20	9.78	31655	0.08	58.9	2.3	158.2
F-1	0.250	0	~0	~0	–	–	–	–
F-2	0.250	12	0.81	2622	0.18	25.3	2.2	156.3
F-3	0.250	20	3.11	10066	0.19	24.2	2.3	155.9

^a Reaction conditions: 50 ml toluene; catalyst: *rac*-Me₂Si[2-Me-4-Ph(Ind)]₂ZrCl₂/MAO catalyst, [Zr] = 1.25×10^{-6} mol, [MAO]/[Zr] = 3000, propylene = 100 psi, temperature = 30 °C, time = 15 min.

^b St-f: St-Cl for runs A and B; St-OSi for runs C and D, St-NSi₂ for runs E and F.

^c Catalyst activity = kg of PP/mol of catalyst · h.

amount of any styrene derivative (St-f) effectively stops the polymerization of propylene. The introduction of hydrogen gradually restores the catalyst activity. Overall, the PP molecular weight is governed by the chain transfer agent – the higher the concentration of the St-f, the lower the molecular weight of the resulting polymer.

Fig. 1 shows the plot of the polymer molecular weight (M_n) versus the molar ratio of [propylene]/[St-f], including three St-Cl/H₂, St-OSi/H₂, and St-NSi₂/H₂ chain transfer agents. In general, the polymer molecular weight and molar ratio of [propylene]/[St-f] are linearly proportional. It is clear that the chain transfer reaction to St-f (with rate constant k_{tr}) is the dominant termination process, and that it competes with the propagating reaction (with rate constant k_p). The degree of polymerization (X_n) follows a simple comparative equation $X_n = k_p[\text{olefin}]/k_{tr}[\text{p-MS}]$ with a chain transfer constant k_{tr}/k_p of 1/21 for St-Cl/H₂, 1/48 for St-OSi/H₂, and 1/34 for St-NSi₂/H₂, respectively. It is intriguing that the k_{tr}/k_p values are significantly lower than those seen in styrene and p-MS cases [11] under similar reaction conditions. The bulky protected functional groups may reduce the frequency of chain transfer reaction. Polymers with very low molecular weights (a few thousand) have been obtained, and the molecular weight distributions are quite narrow, which are generally consistent with single site polymerization processes. Some low

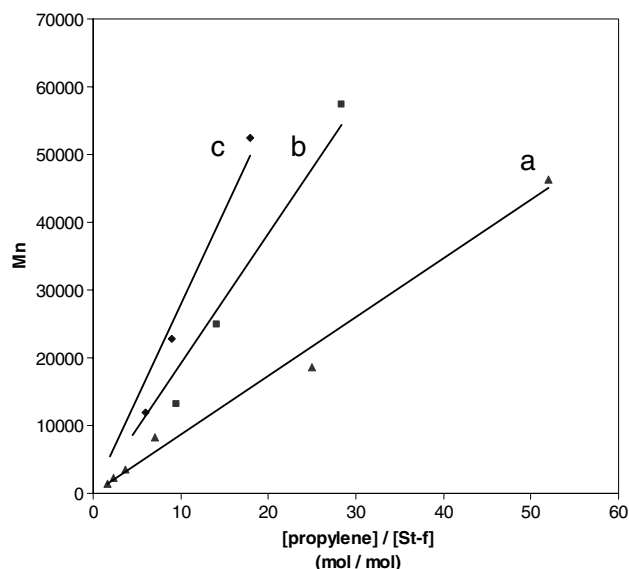


Fig. 1. The plots of number average molecular weights (M_n) of PE-t-St-f polymers vs. the mole ratio of [propylene]/[St-f] using: (a) St-Cl, (b) St-OSi, and (c) St-NSi₂, respectively.

molecular weight polymers with exceptionally low $M_w/M_n < 2$ (despite extra efforts to recover all polymers) may be associated with the sensitivity of GPC at very low molecular range.

The terminal functional group at the polymer chain end provides direct evidence for the chain transfer

reaction. Fig. 2 shows the ^1H NMR spectra (with inset of magnified region and chemical shift assignments) of PP-t-St-OSi polymer and the corresponding PP-t-St-OH. In addition to three major peaks ($\delta = 0.95$, 1.35, and 1.65 ppm) for the CH_3 , CH_2 , and CH groups in the PP backbone, there are three minor chemical shifts at 0.25, 2.61, and 6.75–7.18 ppm (with an intensity ratio near 6/2/4) shown in Fig. 2(a), corresponding to $-\text{OSi}(\text{CH}_3)_2(t\text{-Bu})$, $-\text{CH}_2\text{-}\phi$, and $-\text{CH}_2\text{-C}_6\text{H}_4\text{-OSi}$, respectively. The chemical shift for the silane protecting group completely disappears in Fig. 2(b), indicating the occurrence of a very effective deprotection reaction. The equally split chemical shifts for the phenyl protons, combined with no detectable side product, further indicate the terminal p-alkylphenol moiety.

Fig. 3 compares the ^1H NMR spectra of PP-t-St-NSi₂ polymer ($M_n = 24.2 \times 10^3$; $M_w/M_n = 2.3$) and the corresponding PP-t-St-NH₂. In addition to the chemical shifts for PP polymer, Fig. 3(a) shows all of the chemical shifts associated with the protecting bis(trimethylsilyl)amino terminal group that is connected to the symmetrical p-dialkylbenzene moiety. In fact, all four phenyl protons merge into a single chemical shift at 7.22 ppm. Fig. 3(b) shows an almost identical spectrum, except for the disappearance of the silane protecting group at 0.24 ppm.

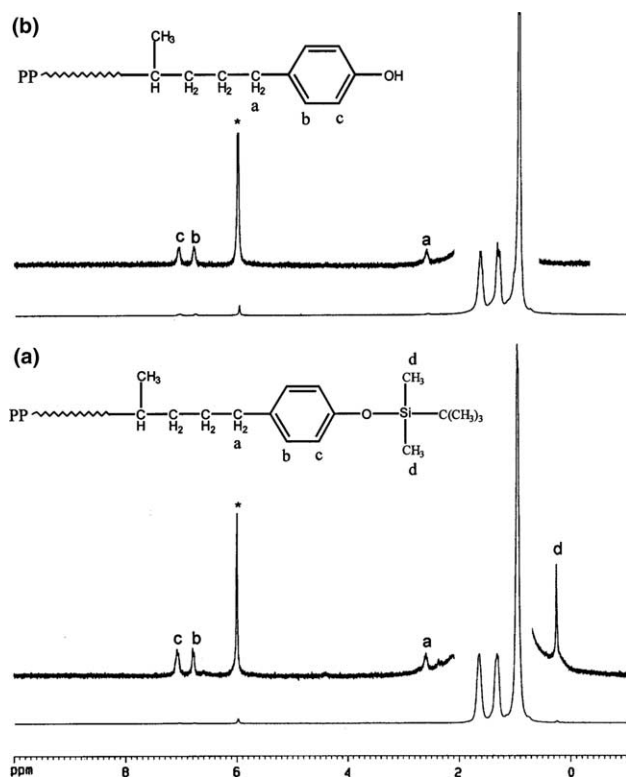


Fig. 2. ^1H NMR spectra of (a) a PP-t-St-OSi polymer and (b) its corresponding PP-t-St-OH. ($M_n = 22000$ g/mol, $M_w/M_n = 2.0$) (solvent: $\text{C}_2\text{D}_2\text{Cl}_4$; temperature: 110°C).

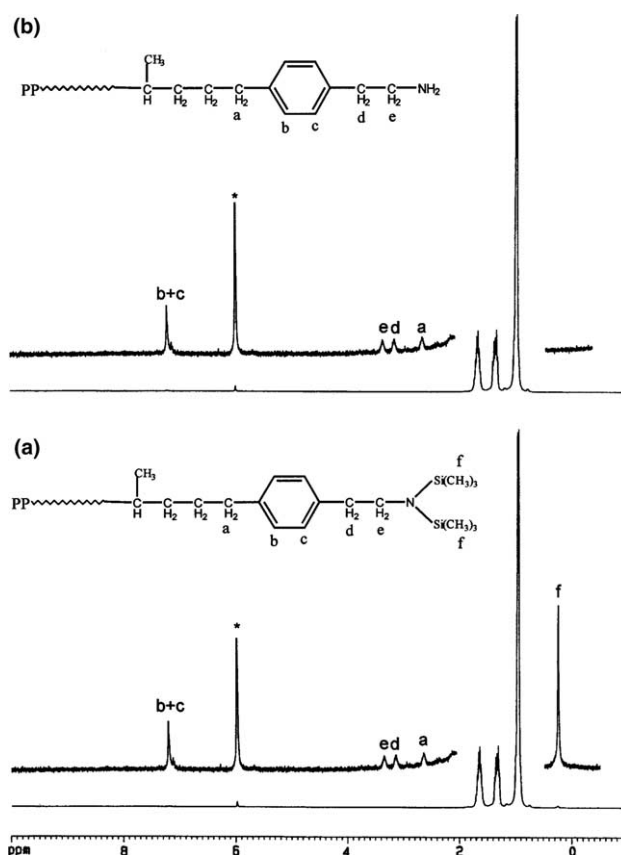


Fig. 3. ^1H NMR spectra of (a) a PP-t-St-NSi₂ polymer and (b) its corresponding PP-t-St-NH₂ ($M_n = 24,200$ g/mol, $M_w/M_n = 2.3$) (solvent: $\text{C}_2\text{D}_2\text{Cl}_4$; temperature: 110°C).

The existence of a terminal functional group in PP was further evidenced by chain extension reaction using the terminal functional group as the reaction site for coupling reaction with polyester and polyamide. Overall, the combined experimental results strongly indicate a clean and effective reaction scheme, as illustrated in Eq. (1). The combination of the facile in situ chain transfer to St-*f*/H₂ during the catalytic polymerization of propylene and the subsequent complete deprotection reaction during the sample work-up step affords a very interesting reaction scheme in the preparation of the chain end functionalized i-PP with a Cl, OH, and NH₂ terminal group via a one-pot reaction process.

3. PP/clay nanocomposites

The availability of a broad range of well-defined functionalized PP polymers provides us with a great advantage in evaluating their applications in PP/clay nanocomposites [12]. The most desirable ammonium group terminated i-PP (PP-t-NH₃⁺Cl⁻) polymers were prepared by simple mixing between PP-t-NH₂ and HCl. Both pristine Na⁺-montmorillonite clay (Na⁺-mmt), with

an ion-exchange capacity of ca. 0.95 mequiv/g, and a dioctadecylammonium-modified montmorillonite organophilic clay (2C18-mmt) were obtained from Southern Clay Products. Static melt intercalation was employed to prepare all PP/clay nanocomposites.

Fig. 4 compares the X-ray diffraction (XRD) patterns before and after static annealing of a physical mixture (90/10 weight ratio) of an ammonium terminated *i*-PP (PP-t-NH₃⁺Cl⁻; $M_n = 58\,900$ and $M_w = 135\,500$ g/mol; $T_m = 158.2$ °C) and a pristine Na⁺-mmt clay. Namely, simple mixing of dried PP-t-NH₃⁺Cl⁻ powder and Na⁺-mmt, ground together by mortar and pestle at ambient temperature, creates the XRD pattern in Fig. 4(a), with a (001) peak at $2\theta \cong 7^\circ$, corresponding to the characteristic Na⁺-mmt d-spacing of ca. 1.26 nm. The mixed powder was then heated – annealed under static conditions – at 190 °C for 2 h under vacuum. The resulting PP-t-NH₃⁺/mmt hybrid shows a featureless XRD pattern in Fig. 4(b), indicating the formation of an exfoliated clay structure, which corresponds to the thermodynamically stable state, as the ammonium-terminated PP exchange the alkali (Na⁺) cations at the mmt surfaces.

Similar featureless patterns were also observed in the PP-t-NH₃⁺Cl⁻/2C₁₈H₃₇-2CH₃-N⁺-mmt nanocomposite cases, suggesting that the dioctadecylammonium cations in organophilic clay may also be ion-exchanged by PP-t-NH₃⁺ to form a similar PP-t-NH₃⁺/mmt structure. It is clear that an organic surfactant is not needed to promote compatibility between PP-t-NH₃⁺Cl⁻ and pristine Na⁺-mmt clay. Beyond any economic benefits, such an elimination of the mmt's organic surfactant, this also offers some significant materials advantages. For example, it eliminates two major concerns relating to the thermal stability of the surfactant during high temperature melt processing and to the long-term stability of the small organic surfactant in the polymer/clay nanocom-

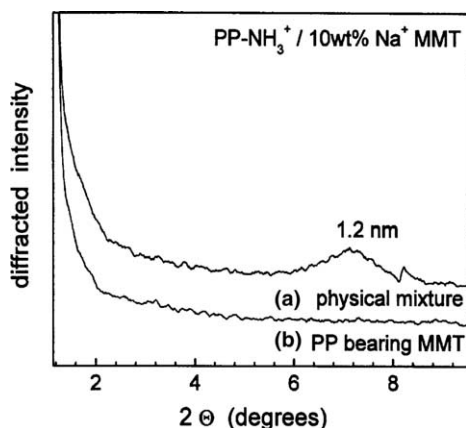


Fig. 4. X-ray diffraction patterns of PP-t-NH₃⁺Cl⁻/Na⁺-mmt (90/10 weight ratio) (a) physical mixture by simple powder mixing at ambient temperature and (b) the same mixture after static melt-intercalation (PP-t-NH₃⁺/mmt hybrid).

posite under various application conditions. The similar results were also observed in other chain functionalized polyolefin cases. The featureless XRD pattern of the melt blending sample clearly shows the exfoliated PP-t-OH/2C18-mmt nanocomposite structure, implying that PP-t-OH is also a good interfacial agent for exfoliating the clay interlayers.

The binary PP-t-NH₃⁺/mmt hybrid was subsequently further mixed/blended (at a 50/50 weight ratio) with a neat –unfunctionalized– *i*-PP ($M_n = 110\,000$ and $M_w = 250\,000$ g/mol). Fig. 5 shows the XRD patterns of (a) the physical mixture and (b) the melt blending, of the exfoliated PP-t-NH₃⁺/mmt structures with neat *i*-PP. The exfoliated structure is maintained after further mixing with *i*-PP, which is compatible (co-crystallizable) with the backbone of the largely-isotactic PP-t-NH₃⁺ polymer, as also directly observed in the TEM image (inset in Fig. 5). Apparently, the *i*-PP polymer chains largely serve as diluents in the ternary PP-t-NH₃⁺/mmt/*i*-PP system, with the thermodynamic stable PP-t-NH₃⁺/mmt exfoliated structure dispersed in the *i*-PP matrix [13].

For comparison, several functionalized PP polymers, containing randomly distributed functional groups in the side chains or lumped together in a block-copolymer microstructure, were also evaluated in PP/montmorillonite nanocomposites. Similar static melt-intercalation procedures were followed, except for employing alkyl-

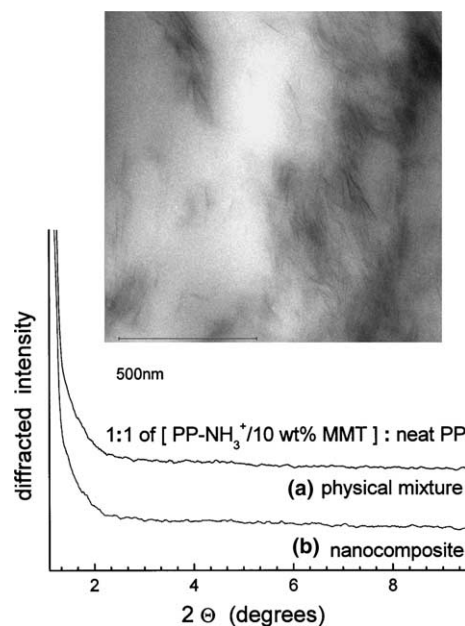


Fig. 5. X-ray diffraction patterns of the 50/50 mixture by weight of exfoliated PP-t-NH₃⁺/mmt structure (90/10 weight ratio) and neat –unfunctionalized– *i*-PP. The XRD traces shown correspond to (a) the physical mixture of PP-t-NH₃⁺/mmt and *i*-PP and (b) the same mixture after static melt-intercalation. Bright-field TEM image of the melt-mixed ternary PP-t-NH₃⁺/mmt/PP system ((b) in the XRD) shows the exfoliated montmorillonite structure.

ammonium-modified montmorillonites (2C18-mmt for all random copolymers, and C18-mmt for the block copolymer). XRD patterns are shown of four nanocomposites made with 6 wt% of 2C18-mmt clay and 94 wt% of three side-chain functionalized PPs ($M_n = 95000$ and $M_w = 210000$ g/mol) containing: (a) 1 mol% p-methylstyrene, (b) 0.5 mol% maleic anhydride, and (c) 0.5 mol% hydroxy side groups, respectively, and the original 2C18-mmt clay. All the functionalized PPs were derived from the same random PP copolymer synthesized by metallocene catalysis, which contained 1 mol% p-methylstyrene (p-MS) comonomer. Subsequently, the p-MS's were selectively functionalized towards hydroxy (OH) and maleic anhydride, respectively, without changing the PP backbone. In addition, we also compared the XRD pattern of PP-*b*-PMMA block copolymer/6 wt% C18-mmt which contains a 5 mol% methyl-methacrylate block. These XRD patterns clearly show that there is a definite intercalated structure for all the side chain functionalized PP cases, manifesting itself through an interlayer d-spacing increase of about 1 nm compared to that of the parent alkyl-ammonium-mmt. TEM was also employed to examine the degree of exfoliated (disordered) structure, and the quantitative image analysis indicates only between 20% and 40% exfoliated layers in all four systems [14].

The experimental results clearly demonstrate the advantage of chain-end-functionalized PP (PP-*t*-NH₃⁺) that seems to adopt a unique molecular structure atop of the clay surfaces and results in an exfoliated montmorillonite structure (Fig. 6(a)). The terminal hydrophilic NH₃⁺ functional group anchors the PP chains (via ion-exchange) on the inorganic surfaces, and the hydrophobic high molecular weight and semi-crystalline PP “tail” effectively exfoliates the clay platelets, an exfoliated structure which is maintained even after further mixing with neat PP. In contrast, side-chain functionalized or

block copolymer PPs form multiple contacts with each of the clay surfaces, as illustrated in Fig. 6(b), which not only results in aligning the polymer chains parallel to the clay surfaces, but can also bridge consecutive clay platelets promoting intercalated structures, especially for the higher lateral size montmorillonites.

4. Experimental

All manipulations were carried out under inert atmosphere or by using standard Schlenk technique. ¹H NMR was measured on a Bruker AM-300 or WM-360 spectrometer with DISNMR software. The measurements were usually taken at 120 °C using d₂-1,1,2,2-tetrachloroethane as solvent. The molecular weight and molecular weight distribution of the polymers were determined by gel permeation chromatography (GPC) using a Waters 150 C with a refractive index (RI) detector. The measurements were taken at 140 °C using 1,2,4-trichlorobenzene (TCB) as solvent and a mobile phase of 0.7 ml/min flow rate. Broad molecular weight PE samples were used as standards for calibration. Differential scanning calorimetry (DSC) was measured on a Perkin-Elmer DSC-7 instrument controller. The DSC curves were recorded during the second heating cycle from 30° to 180 °C with a heating rate of 20 °C/min. XRD data were collected on a diffractometer using Cu K α radiation ($\lambda = 0.1506$ nm). Bragg's law ($\lambda = 2d\sin\theta$) was used to calculate the spacing. Direct observation of the PP/clay nanocomposite structure was realized by bright field TEM of nanocomposite films under strain in a JEOL -1200EX operating at 120 kV. Ultrathin sections of the PP/clay with a thickness of approximately 50 nm were prepared at room temperature using an ultramicrotome equipped with a diamond knife. The sections were transferred dry to carbon-coated Cu grids of 200 mesh.

Me₂Si(2-methyl-4-phenyl-indenyl)₂ZrCl₂ (Boulder Scientific Co.) was used as received. MAO (Albemarle) in 30 wt% of solution in toluene was isolated by vacuum removal of toluene and re-compounded to 2.5 M toluene solution prior to use. CP grade propylene gas (MG Industries) was dried over CaH₂ prior to use. CP grade toluene, hexane, and THF were deoxygenated by argon purge before refluxing for 48 h and then distilled over sodium benzophenone right before use.

4.1. Synthesis of 4-(*t*-butyldimethylsilyloxy)styrene (*St*-OSi)

4-(*t*-Butyldimethylsilyloxy)styrene was synthesized in two steps. In a 500 ml flask equipped with a magnetic stirring bar, 70.4 g (1.02 mol) of imidazole was mixed with 52.4 g (0.42 mol) of 4-hydroxybenzaldehyde and

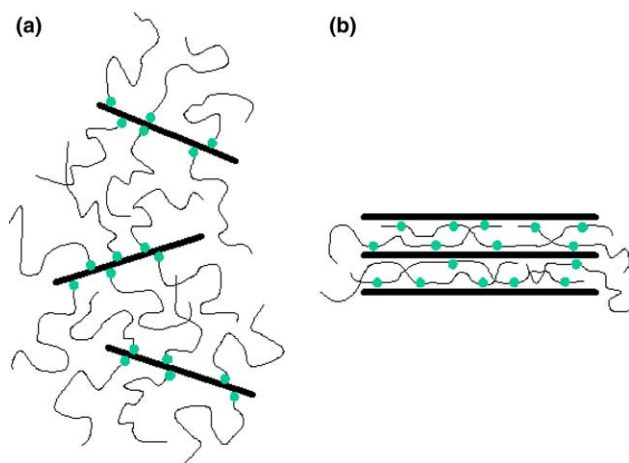


Fig. 6. Illustration of the molecular structures of (a) chain end functionalized and (b) side chain functionalized polyolefin located between clay interlayers.

77.4 g (0.52 mol) of *t*-butyldimethylsilyl chloride in THF solution. The mixture was stirred at ambient temperature for 4 h before being poured into cold water. The organic layer was separated and extracted with ether, then dried with magnesium sulfate. About 94 g of 4-(*t*-butyldimethylsilyloxy)benzaldehyde (90% yield) was obtained after evaporating the solvent. The second reaction step was performed under a nitrogen atmosphere. In a 500 ml flask equipped with a magnetic stirring bar, 123.6 g (0.38 mol) of methyltriphenylphosphonium bromide suspended in THF was treated with 149.6 ml (0.19 mol) of *n*-butyllithium (2.5 M in hexane). After 1 h, 80.0 g (0.34 mol) of 4-(*t*-butyldimethylsilyloxy)benzaldehyde was introduced dropwise into the red solution. The mixture was stirred overnight at room temperature and then poured into cold water. The organic layer was separated by ether extraction and dried with magnesium sulfate. Further purification was performed by distillation under vacuum (10 Torr) at elevated temperature (80 °C). 65 g of 4-(*t*-butyldimethylsilyloxy)styrene was obtained with a yield of more than 90%.

4.2. Synthesis of 4-{2-[*N,N*-bis(trimethylsilyl)amino]ethyl}styrene (*p*-NSi₂-St)

A silane protected chain transfer agent *p*-NSi₂-St was prepared in two steps. In a 500 ml flask equipped with a magnetic stirring bar, 100 g of lithium bis(trimethylsilyl)amide dissolved in 200 ml of THF was slowly added into a mixture of 50 ml (0.658 mol) of chloromethyl methyl ether and 50 ml of THF at 0 °C under a nitrogen atmosphere. After completing the addition, the solution was allowed to warm up to room temperature for 2 h before evaporating the excess chloromethyl methyl ether and THF solvent. *N,N*-Bis(trimethylsilyl)methoxymethylamine (80% yield) was isolated by distillation. In the second step, *p*-NSi₂-St was prepared by treating 4-vinylbenzylmagnesium chloride with *N,N*-bis(trimethylsilyl)methoxymethylamine. In a 500 ml flask equipped with a magnetic stirring bar and a condenser, 15.2 g of magnesium was suspended in 50 ml dry ether, and 80 ml of 4-vinylbenzyl chloride diluted with 50 ml dry ether was then introduced dropwise through the condenser. The solution was refluxed for 4 h before the addition of 117 g of *N,N*-bis(trimethylsilyl)methoxymethylamine over a period of 2 h. The reaction was allowed to proceed at room temperature for another 2 h before adding 100 ml of aqueous NaOH solution (30%). The organic layer was separated and dried, and the residual was then distilled over CaH₂ to obtain *p*-NSi₂-St with 70% yield.

4.3. Synthesis of NH₂ group terminated PP (*PP-t-NH*₂)

The *p*-NSi₂-St terminated PP polymers (*PP-t-St-NSi*₂) were prepared by the combination of *rac*-Me₂Si[2-Me-4-

Ph(Ind)₂ZrCl₂/MAO catalyst and *p*-NSi₂-St and H₂ as the chain transfer agents. A systematic study was conducted to evaluate the effects of *p*-NSi₂-St and H₂ concentrations on the catalyst activity and polymer molecular weight. The *PP-t-NH*₂ polymers were then prepared from *PP-t-St-NSi*₂ polymers by treating them with hydrogen chloride, which can be accomplished during the sample work-up step. Alternatively, the isolated *PP-t-St-NSi*₂ (2 g) was suspended in 50 ml of THF at 50 °C before adding dropwise 2 N methanolic hydrogen chloride solution. The mixture was stirred for 4 h at 50 °C, and then poured into 1 N methanolic NaOH solution. The *PP-t-NH*₂ polymer was collected by filtration and washed with 1 M aqueous ammonia and water under a nitrogen atmosphere. The polymer was dried overnight at 50 °C under vacuum. The *PP-t-NH*₂ polymer yield was quantitative. Overall, the *PP-t-NH*₂ molecular weight is governed by the chain transfer agent – the higher the concentration of the *p*-NSi₂-St, the lower the molecular weight of the resulting polymer. It is clear that the chain transfer reaction to *p*-NSi₂-St (with rate constant *k*_{tr}) is the dominant termination process, and that it competes with the propagating reaction (with rate constant *k*_p). The degree of polymerization (*X*_n) follows a simple comparative equation $X_n = k_p[\text{olefin}]/k_{tr}[\text{St-NSi}_2]$ with a chain transfer constant of *k*_{tr}/*k*_p = 1/34. ¹H NMR spectra of *PP-t-St-NSi*₂ polymer and the corresponding *PP-t-St-NH*₂ show clean deprotection reaction with the complete disappearance of the silane protecting group at 0.24 ppm.

4.4. Preparation of *PP/PP-t-NH*₃⁺Cl⁻/Na⁺-montmorillonite clay nanocomposite

Na⁺-montmorillonite clay (Na⁺-mmt) with an ion-exchange capacity of ca. 95 mequiv/100 g (WM) was obtained from Southern Clay Product. *PP-t-NH*₃⁺Cl⁻ (*T*_m = 158.2 °C; *M*_n = 58,900 and *M*_w = 135,500 g/mol) was prepared using excess HCl reagent. Static melt intercalation was employed to prepare *PP-t-NH*₃⁺Cl⁻/Na⁺-montmorillonite nanocomposite. *PP-t-NH*₃⁺Cl⁻ dried powder and Na⁺-mmt with 90/10 weight ratio were first mixed and ground together in a mortar and pestle at ambient temperature. The XRD pattern of this simple mixture shows a (001) peak at 2θ ~ 7, corresponding to Na⁺-mmt interlayer structure with a d-spacing of 1.45 nm. The mixed powder was then heated at 190 °C for 2 h under nitrogen condition. The resulting *PP-t-NH*₃⁺Cl⁻/Na⁺-mmt nanocomposite shows a featureless XRD pattern, indicating the formation of an exfoliated clay structure.

The binary *PP-t-NH*₃⁺Cl⁻/Na⁺-mmt exfoliated nanocomposite was further melt mixed (50/50 weight ratio) with commercial neat *i*-PP (*M*_n = 110,000 and *M*_w = 250,000 g/mol). First, the *PP-t-NH*₃⁺Cl⁻/Na⁺-mmt exfoliated nanocomposite and neat *i*-PP with 50/50 weight ratio were ground together in a mortar and pestle at

ambient temperature. This simple mixture shows a featureless XRD pattern. The mixed powder was then heated at 190 °C for 2 h under nitrogen condition. The resulting ternary PP/PP-t-NH₃⁺Cl⁻/Na⁺-mmt nanocomposite also shows a featureless XRD pattern, indicating that the stable exfoliated structure in the binary PP-t-NH₃⁺Cl⁻/Na⁺-mmt exfoliated nanocomposite is clearly maintained after further mixing with PP that is compatible with the backbone of PP-t-NH₃⁺Cl⁻.

5. Conclusion

We have shown a one-pot process to prepare chain end functionalized PP polymers, involving metallo-cene-mediated propylene polymerization/chain transfer reaction. With the proper choice of reaction conditions, chain transfer agents, and catalyst system, it is very convenient and efficient (with high catalyst activity) to prepare i-PP with a terminal styrenic unit containing either an OH or NH₂ group. This reaction scheme is especially useful in the preparation of chain-end functionalized PP with high molecular weight. Almost the same reaction procedures used in regular PP polymerization can be directly applied, except for the addition of a small amount of chain transfer agent. In turn, the PP polymer with a reactive functional group is a useful interfacial material that can be used as polymeric surfactant to prepare the exfoliated PP/clay nanocomposites.

Acknowledgments

The authors would like to thank the Office of Naval Research and the National Institute of Standards and Technology for their financial support.

References

- [1] T.C. Chung, Functionalization of Polyolefins, Academic Press, London, 2002.
- [2] (a) D. Napper, Polymeric stabilization of colloidal dispersions, Academic Press, London, 1983;
(b) A. Gast, L. Leibler, *Macromolecules* 19 (1986) 686;
(c) L.H. Lee, Adhesion and adsorption of polymers, Plenum Press, New York, 1980.
- [3] (a) C. Koning, M. Van Duin, C. Pagnoulle, R. Jerome, *Prog. Polym. Sci.* 23 (1998) 707;
(b) J. Noolandi, K.M. Hong, *Macromolecules* 15 (1982) 482;
(c) S.T. Milner, H. Xi, *J. Rheol.* 40 (1996) 663.
- [4] T.C. Chung, *ChemTech* 27 (1991) 496.
- [5] (a) C.H. Bamford, A.D. Jenkins, R.P. Wayne, *Trans. Faraday Soc.* 56 (1960) 932;
(b) H.C. Haas, N.W. Schuler, H.S. Kolesinski, *J. Polym. Sci. Part A1* 5 (1967) 2964.
- [6] (a) H. Brody, D.H. Richards, M. Szwarc, *Chem. Ind.* (1958) 1473;
(b) K. Hayashi, C.S. Marvel, *J. Polym. Sci. Part A1* 2 (1974) 2571;
(c) M. Morton, L.J. Fetters, J. Inomater, D.C. Rubio, R.N. Young, *Rubber Chem. Technol.* 49 (1976) 303.
- [7] (a) H. Yasuda, M. Furo, H. Yamamoto, A. Nakamura, S. Miyake, N. Kibino, *Macromolecules* 25 (1992) 5115;
(b) M. Brookhart, J.M. Desimone, B.E. Grant, M.J. Tanner, *Macromolecules* 28 (1995) 5378;
(c) K.J. Shea, J.W. Walker, H. Zhu, M. Paz, J. Greaves, *J. Am. Chem. Soc.* 911 (1997) 9049;
(d) G. Desurmont, T. Tokimitsu, H. Yasuda, *Macromolecules* 33 (2000) 7679.
- [8] T.C. Chung, *Prog. Polym. Sci.* 27 (2002) 39.
- [9] (a) G. Xu, T.C. Chung, *J. Am. Chem. Soc.* 121 (1999) 6763;
(b) G. Xu, T.C. Chung, *Macromolecules* 32 (1999) 8689;
(c) T.C. Chung, G. Xu, Yingying Lu, Youliang Hu, *Macromolecules* 34 (2001) 8040.
- [10] (a) T.C. Chung, J.Y. Dong, *J. Am. Chem. Soc.* 123 (2001) 4871;
(b) J.Y. Dong, T.C. Chung, *Macromolecules* 35 (2002) 1622.
- [11] (a) J.Y. Dong, Z.M. Wang, H. Han, T.C. Chung, *Macromolecules* 35 (2002) 9352;
(b) T.C. Chung, J.Y. Dong, U.S. Patent 6,479,600 (2002).
- [12] Z.M. Wang, H. Nakajima, E. Manias, T.C. Chung, *Macromolecules* 36 (2003) 8919.
- [13] (a) R. Krishnamoorti, E.P. Giannelis, *Langmuir* 17 (2001) 1448;
(b) R. Krishnamoorti, J.X. Ren, A.S. Silva, *J. Chem. Phys.* 114 (2001) 4968;
(c) J.X. Ren, B.F. Casanueva, C.A. Mitchell, R. Krishnamoorti, *Macromolecules* 36 (2003) 4188.
- [14] E. Manias, A. Touny, L. Wu, K. Strawhecker, B. Lu, T.C. Chung, *Chem. Mater.* 13 (2001) 3516.